ORIGINAL RESEARCH

Beneficial Effect of Selenium Doped Carbon Quantum Dots Supplementation on the in vitro Development Competence of Ovine Oocytes

Mengqi Wang[1],*, Jingyu Ren[1],*, Zhanpeng Liu[2], Shubin Li[3], Liya Su[1], Biao Wang[4], Daoning Han[1], Gang Liu [1]

[1]Key Laboratory of Medical Cell Biology, Clinical Medicine Research Center, Affiliated Hospital of Inner Mongolia Medical University, Hohhot, Inner Mongolia, People's Republic of China; [2]College of Life Science, Inner Mongolia University, Hohhot, Inner Mongolia, People's Republic of China; [3]Department of Geriatric Medical Center, Inner Mongolia People's Hospital, Hohhot, Inner Mongolia, People's Republic of China; [4]Animal Husbandry Institute, Inner Mongolia Academy of Agricultural & Animal Husbandry Sciences, Hohhot, Inner Mongolia, People's Republic of China

*These authors contributed equally to this work

Correspondence: Gang Liu, Email 21408010@mail.imu.edu.cn

Background: After the synthesis of selenium doped carbon quantum dots (Se/CDs) via a step-by-step hydrothermal synthesis method with diphenyl diselenide (DPDSe) as precursor, the beneficial effects of Se/CDs' supplementation on the in vitro development competence of ovine oocytes were firstly investigated in this study by the assay of maturation rate, cortical granules' (CGs) dynamics, mitochondrial activity, reactive oxygen species (ROS) production, epigenetic modification, transcript profile, and embryonic development competence.

Results: The results showed that the Se/CDs' supplementation during the in vitro maturation (IVM) process not only enhanced the maturation rate, CGs' dynamics, mitochondrial activity and embryonic developmental competence of ovine oocytes, but remarkably decreased the ROS production level of ovine oocytes. In addition, the expression levels of H3K9me3 and H3K27me3 in the ovine oocytes were significantly up-regulated after the Se/CDs' supplementation, in consistent with the expression levels of 5mC and 5hmC. Moreover, 2994 up-regulated differentially expressed genes (DEGs) and 846 repressed DEGs were found in the oocytes after the Se/CDs' supplementation. According to the analyses of Gene Ontology (GO) and Kyoto Encyclopedia of Genes and Genomes (KEGG), these DEGs induced by the Se/CDs' supplementation were positively related to the progesterone mediated oocyte maturation and mitochondrial functions. And these remarkably up-regulated expression levels of DEGs related to oocyte maturation, mitochondrial function, and epigenetic modification induced by the Se/CDs' supplementation further confirmed the beneficial effect of Se/CDs' supplementation on the in vitro development competence of ovine oocytes.

Conclusion: The Se/CDs prepared in our study significantly promoted the in vitro development competence of ovine oocytes, benefiting the extended research about the potential applications of Se/CDs in mammalian breeding technologies.

Keywords: Se/CDs, mitochondrial activity, reactive oxygen species production, ovine oocytes and transcript profiles

Background

In 1878, the first case of in vitro fertilization (IVF) was conducted by Schenk with the first documented birth of rabbit via the technology of IVF-embryo transfer (ET) achieved by Walter Heape in 1959,[1] benefiting the applications of assisted reproductive technologies (ARTs) in mammalian breeding via the in vitro production (IVP) of mammalian embryos during the past decades. With the promising development of ARTs, the technologies including ovum pick-up (OPU), in vitro maturation (IVM), IVF, cryobiology of mammalian gametes and ET not only promote these in vitro research related to gametogenesis, stem cells, and developmental biology,[2] but also offer new alternatives for the fertility preservation for patients undergoing cancer treatments and reproductive failures.

Nevertheless, the ARTs applied for livestock and human beings lack the complex ovarian microenvironments in vivo, which are necessary for the in vivo processes of oogenesis, granulogenesis, oocyte maturation, ovulation, and steroidogenesis.[3] The complex ovarian microenvironments in vivo are strictly regulated by the physiological changes (functional or structural changes) in mammalian ovaries.[4] And the deficiency of in vivo ovarian microenvironments including gonadotropins, intra/extraovarian factors, pH, osmolarity and mechanical stress[5] during the IVM process disturbs the mitochondrial functions, further triggering the failures of oocyte maturation and decreased fertilization potential. In addition, numerous studies have found that the mitochondrial dysfunctions during the IVM process cause the excessive production and accumulation of reactive oxygen species (ROS) via the process of oxidative phosphorylation,[6] resulting in intracytoplasmic oxidative stress related damage and physiological disorders of oocyte development.[7]

As the most abundant organelle in mammalian oocytes, mitochondria play an important role in the oocyte maturation and ovulation via the generation of adenosine triphosphate (ATP) and secretion of fatty acid β-oxidation.[8] Meanwhile, the mitochondrial dysfunctions during the oocyte maturation, due to the exposure to chemotherapeutics,[8] ionizing radiation,[9] toxic metals,[10] plasticizers,[11] pesticides[12] and polycyclic aromatic hydrocarbons are positively related to mammalian infertility and chromosomally abnormal conception.[13] These former publications have also found that the mitochondrial dysfunctions during the toxic metals exposure process altered the epigenetic modifications including 5-methylcytosine (5mC) methylation and H3, lysine 9 trimethylation (H3K9me3), resulting in the following embryonic development failures and transgenerational genotoxicity.[14–17]

According to the positive connections between the developmental failures of mammalian oocytes and mitochondrial dysfunctions, the supplementation of antioxidant substances including melatonin, vitamin C, quercetin, and coenzyme Q10 has been reported to have a beneficial effect on the efficiency of mammalian IVM via the inhibition of mitochondrial dysfunctions.[18–20] Furthermore, these recent advances in the converging technologies among nanotechnology, biotechnology, and information technology provide exciting alternatives for developing novel broad-spectrum platforms to promote the outcomes of mammalian IVM via restraining the mitochondrial dysfunctions and intracellular ROS accumulation.[21–23] And the potential applications of nanominerals, particularly selenium nano-particles (SeNPs) and zinc nanoparticles (ZnNPs) on the production, immunity, and reproduction abilities of animals have already been confirmed.[24] These former literature also confirmed the beneficial effect of SeNPs' supplementation on the IVM efficiency of bovine oocytes via the up-regulation of antioxidant defense and inhibition of mitochondrial dysfunctions.[21,25] However, the potential effects of carbon quantum dots (CDs) doped with trace elements (including selenium, zinc and boron) on the efficiency of mammalian IVM remain unreported.

In the present study, the synthesis of selenium (Se) doped carbon quantum dots (Se/CDs) via a step-by-step hydrothermal synthesis method was conducted with diphenyl diselenide (DPDSe) as precursor and the effect of Se/CDs' supplementation on the in vitro development competence of ovine oocytes including maturation rate, cortical granules (CGs) dynamics, mitochondrial activity, ROS production, epigenetic modification, and transcript profile was investigated for the first time. Furthermore, the fertilization competence of ovine oocytes after Se/CDs' supplementation was finally analyzed to confirm the potential effect of Se/CDs' supplementation on the IVM of ovine oocytes.

Methods
Chemicals
Unless otherwise indicated, the commercial chemicals, medium and supplements applied in the following study were purchased from Sigma Aldrich (Shanghai, China) and Thermo Fisher Scientific (Shanghai, China).

Synthesis of Se/CDs
Se/CDs were synthesized by a step-by-step hydrothermal synthesis method. Firstly, 400 mg of diphenyl diselenide (DPDSe, Heowns, Tianjin, China) was dissolved into 30 mL of ethanol (Aladdin, Shanghai, China) with the mixture heated at 120°C°C for 20 h to prepare the precursor. After heating, 800 mg of citric acid (Aladdin, Shanghai, China) was added to the previously-mentioned precursor, followed by a subsequent incubation at 200°C for 10 h. Then, 800 mg of urea (General-Reagent, Tianjin, China) was added to the mixture and heated at 200°C for 10 h. The solution was cooled

to room temperature with the precipitate removed by centrifugation at 8000 rpm for 20 min, and the previously-mentioned processes were repeated three times. After centrifugation, the supernatant was collected with the excessive liquid spanned off and dialyzed for 24 h by a 1000 kDa dialysis bag (Solarbio, Beijing, China). The mixtures were freeze-dried for a subsequent 48 h.

Characterization of Se/CDs

For the characterization of Se/CDs, the transmission electron microscopy (TEM) images were prepared by a JEOL JEM-2100F Field Transmission Electron Microscope (Tokyo, JAPAN). The X-ray diffraction (XRD) pattern was measured by a Bruker D8 Focus Diffraction System with Cu Ka radiation (λ= 0.15406 nm). The X-ray Photoelectron Spectroscopy (XPS) analysis was observed by a Thermo Fisher Scientific Escalab 250Xi using Al monochromatic Ka radiation (hv = 1486.6 eV) with the binding energies of the C 1s line at 284.8 eV from adventitious carbon. The UV spectrum of Se/CDs was examined by OCEAN OPTICS (DH-2000-BAL). The photoluminescence (PL) of the aqueous solution was measured by F-380 with the exit and entrance slit set as 5 nm. Fourier transform infrared (FT-IR) spectrum was recorded by the ALPHA FT-IR spectro-photometer from 370 to 7500 cm^{-1} using the infrared reflection method.

COCs Collection

The ovine ovaries were collected from a local slaughterhouse, kept in 30°C pre-warmed normal saline supplemented with 100 μg/mL penicillin and 100 μg/mL streptomycin solution (P/S, 15,140,122, Thermo Fisher Scientific, Shanghai, China) and transported to the laboratory within 2 h. Upon the ovaries' arrival, the ovaries were thoroughly washed with 37°C pre-warmed normal saline with the collections of cumulus oocyte complexes (COCs) conducted based on the department's protocols.[3]

Briefly, the ovine ovaries were placed in 100 mm sterile dishes (Nunc, Beijing, China) supplemented with 15 mL dissecting solution TCM-199 medium (11,150,067, Thermo Fisher Scientific, Shanghai, China) containing 4 mg/mL bovine serum albumin (BSA, A3803, Sigma Aldrich, Shanghai, China), 1% Hepes (15,630, Thermo Fisher Scientific, Shanghai, China), 2 μg/mL heparin sodium (CH6021, Coolaber, Beijing, China), and 100 μg/mL P/S. After COCs' release from the ovaries with sterilized forceps and surgical blades, all COCs were microscopically picked up and these COCs with even cytoplasm of oocytes and approximately three to four layers of cumulus cells were collected for the following IVM.[3]

IVM, Se/CDs' Supplementation and Experimental Group Setting

The IVM medium applied in this study was TCM-199 medium containing 100 μM cysteamine (M9768, Sigma Aldrich, Shanghai, China), 10 ng/mL epidermal growth factor (EGF,31509, PEPRO TECH, Hangzhou, China), 10% fetal bovine serum (FBS, 30,044,333, Thermo Fisher Scientific, Shanghai, China), 10 U/mL follicle stimulating hormone (FSH, Ningbo Sansheng, Ningbo, China), 2 mM Gluta^{MAX} (35,050,061, Thermo Fisher Scientific, Shanghai, China), 10 U/mL luteinizing hormone (LH, Ningbo Sansheng, Ningbo, China), 0.3 mM sodium pyruvate (11,360,070, Thermo Fisher Scientific, Shanghai, China), and 1 μg/mL β-2-oestradiol (E8875, Sigma Aldrich, Shanghai, China).

During the IVM process, different concentrations of Se/CDs, dissolved in TCM-199 medium, were added to the IVM medium with the experimental setting designed as follows: the negative control group (NC group) with the supplementation of TCM-199 medium, LD group with the supplementation of 50 μg/mL Se/CDs, MD group with the supplementation of 100 μg/mL Se/CDs, and HD group with the supplementation of 200 μg/mL Se/CDs, respectively.

According to the experimental group setting, COCs were randomly collected (repeated in triplicate), transferred to 500 μL of IVM medium drops (30–40 COCs per drop) covered with mineral oil (M8410, Sigma Aldrich, Shanghai, China) in a 4-well culture dish (Corning, Beijing, China) and cultured at 38.5°C, 5% CO_2 for the following 24 h.

Assessment of IVM Efficiency

After IVM, the assessment of IVM efficiency was conducted according to the department protocol.[3] Briefly, COCs after IVM of each group (n=110 for the NC group, n=110 for the LD group, n=110 for the MD group and n=113 for the HD group, repeated in triplicate) were individually treated with 400 IU/mL hyaluronidase solution (H3506, Sigma Aldrich, Shanghai, China) at 38.5°C for 3 min and repeatedly pipetted to remove the cumulus cells. Subsequently, these COCs were washed thoroughly with the Hepes-synthetical oviductal fluid (H-SOF) medium to obtain the denuded oocytes.

After collection, the denuded oocytes of each group were microscopically examined with the first polar body extrusion (PBE) rate, as the maturation rate of each group was further analyzed. In addition, the denuded oocytes at the metaphase II (MII) stage of each group were selected for the following experiments.

Toxicity Effect Assessment of Se/CDs

To assess the toxicity effect of Se/CDs' supplementation on the in vitro development competence of ovine oocytes, the denuded oocytes of each group after IVM (n= 114 for the NC group, n=123 for the LD group, n=113 for the MD group and n=121 for the HD group, repeated in triplicate) were collected with the oocytes' fragmentation rates of each group microscopically examined.

Moreover, the cumulus cells of each group after IVM (repeated in triplicate) were collected with 2×10^3 cells of each group added to 96-well plate (Corning, Beijing, China) and cultured with the DMEM/F12 medium (11,320,033, Gibco, Shanghai, China) supplemented with 10% FBS and 100 μg/mL P/S at 38.5°C, 5% CO_2 overnight. According to the manufacturer's instructions for a CCK-8 proliferation detection kit (C0037, Beyotime, Beijing, China), 10 μL of CCK-8 reagent was added to each well. After subsequent incubation for 1 h, the absorbance of each well at 450 nm was recorded by Multiskan GO system (Thermo Fisher Scientific, China).[26]

Cortical Granules' (CGs) Dynamics Assay

To analyze the potential effect of Se/CDs' supplementation on the cytoplasmic maturation of ovine MII oocytes, the cortical granules' (CGs) dynamics assay of ovine MII oocytes was performed.[17,27]

Briefly, MII oocytes of each group (n=30, repeated in triplicate) were collected, fixed in 4% paraformaldehyde solution (PFA, P1110, Solarbio, Beijing, China) for 30 min and permeabilized in 0.5% Triton X-100 solution (T8200, Solarbio, Beijing, China) for 15 min. Subsequently, the oocytes were incubated with 1% BSA solution (SW3015, Solarbio, Beijing, China) for 30 min and labeled with a fluorescein labeled lens culinaris agglutinin (LCA-FITC, FL-1041, Vector Laboratories, CA, USA) at 4°C for 2 h according to the manufacturer's instructions.

After LCA-FITC staining, the oocytes of each group were collected, washed with Dulbecco's phosphate buffered saline (DPBS, 14,190,250, Thermo Fisher Scientific, Beijing, China) containing 1% Tween 20 solution (T8220, Solaribo, Beijing, China), mounted on glass slides, and examined under a confocal microscope (A1R, Nikon, Tokyo, Japan) with the LCA-FITC staining densities of each group analyzed with Image J software.[27]

Mitochondrial Activity Analysis

To analyze the potential effect of Se/CDs' supplementation on the mitochondrial activity of ovine MII oocytes, MitoTracker staining of ovine MII oocytes was conducted.[17]

Briefly, MII oocytes of each group (n=30, repeated in triplicate) were collected, washed thoroughly with DPBS and subsequently incubated with 200 nM MitoTracker Red CMXRos working solution (C1049, Beyotime, Haimen, China) for 30 min according to the manufacturer's instructions. After MitoTracker Red CMXRos staining and microscopical examination, the MitoTracker staining densities of each group were assessed with Image J software.[27]

Assay of ROS Production Levels

For the assay of ROS production levels, MII oocytes of each group (n=30, repeated in triplicate) were collected, washed with DPBS, and subsequently incubated with 10 μM dichlorofluorescein diacetate solution (DCFH-DA, S0033, Beyotime, Haimen, China) for 30 min according to the department's protocols.[3] After microscopical examination, the DCFH-DA staining densities of each group were calculated with Image J software.[27]

Immunofluorescence Staining of Epigenetic Modifications

After fixation, permeabilization, and BSA blocking, MII oocytes (n=30, repeated in triplicate) of each group were immunostained for the epigenetic modification analyses (histone methylation and DNA methylation) according to the department's protocols with small modifications.[3,28]

After incubation of primary antibodies including a rabbit polyclonal anti-H3K9me3 antibody (with 1:500 dilutions in 5% BSA, ab176916, Abcam, Shanghai, China), a rabbit polyclonal anti-H3K27me3 antibody (with 1:300 dilutions in 5% BSA, ab192985, Abcam, Shanghai, China), a rabbit anti-5mC antibody (with 1:500 dilutions in DPBS, ab214727, Abcam, Shanghai, China) and a rabbit polyclonal anti-5hmC antibody (with 1:500 dilutions in 5% BSA, ab214728, Abcam, Shanghai, China) at 4°C overnight, the oocytes of each group were thoroughly washed with DPBS and incubated with the corresponding secondary antibodies such as an Alexa Fluor® 647 secondary antibody (specific for H3K9me3, H3K27me3 and 5mC, with 1:300 dilutions in DPBS, ab150075, Abcam, Shanghai, China) and an Alexa Fluor® 555 secondary antibody (specific for 5hmC, with 1:300 dilutions in DPBS, ab150074, Abcam, Shanghai, China) at room temperature for 1 h.

After being washed three times with DPBS, the immunostained oocytes were collected and individually re-incubated with 5 μg/mL Hoechst 33,342 solution (B8040, Solarbio, Beijing, China) for 5 min, followed by the oocytes' mounting and microscopical examination with the staining intensity of each group analyzed with Image J software.

Smart-Seq Analyses

For the RNA extraction, library construction and sequencing, ovine MII oocytes from the NC and MD groups (n=50) were lysed with 10 × Lysis Buffer (N711, Vazyme, Nanjing, China). To generate the Smart-Seq library, priming buffer mix containing dNTPs and oligo-dT primers was added to the oocyte lysate and denatured at 72°C. cDNA synthesis and pre-amplification of cDNA was performed using the Discover-SC WTA Kit (N711-01, Vazyme, Nanjing, China) according to the manufacturer's instructions.

Subsequently, cDNA of ovine oocytes were purified with VAHTS DNA Clean Beads with the sequencing libraries constructed according to the manufacturer's instructions of TruePrepTM DNA Library Prep Kit (TD503, Vazyme, Nanjing, China). Lastly, the library quality was assessed by an Agilent 2100 Bioanalyzer (Agilent Technologies, Palo Alto, CA, USA) and sequenced using Illumina HiSeq2500 by Gene Denovo Biotechnology Co. (Guangzhou, China).

For the bioinformatic analyses between the NC and MD groups, the filtering of clean reads, alignment with Ribosome RNA (rRNA) and alignment with ovine reference genome were conducted, followed by the quantification of gene abundance conducted by the value of fragment per kilobase of transcript per million mapped reads (FPKM).[29] In addition, the RNAs differential expression analysis was performed by DESeq2 software between the NC and MD groups. The genes with the parameter of false discovery rate (FDR) below 0.05 and absolute fold change≥2 were considered as the differentially expressed genes (DEGs), followed by the GO analyses[30] and pathway enrichment analyses by Kyoto Encyclopedia of Genes and Genomes (KEGG).[31]

IVF and Fertilization Potentials' Assessment

To analyze the effect of Se/CDs' supplementation on the fertilization potentials of ovine MII oocytes, the fertilization potentials' assessment of MII oocytes was performed according to the department's protocols.[3,17]

Briefly, MII oocytes of each group (n=221 for the NC group, n=218 for the LD group, n=220 for the MD group and n=229 for the HD group, repeated in triplicate) were collected and individually transferred into 500 μL of fertilization medium such as SOF medium containing 1 mM caffeine (58,082, Amresco, Shanghai, China), 10 μg/mL heparin sodium, 2% oestrus ovine serum and 2 mM sodium pyruvate and cultured in a CO_2 incubator (38.5°C, 5% O_2 and 5% CO_2). The thawing of frozen semen straws (LEKE, Hohhot, Inner Mongolia, China) and collection of spermatozoa were performed,[32] followed by the transfer of spermatozoa with the final concentration of $1×10^6$ sperm/mL to the previously-mentioned fertilization medium containing MII oocytes and insemination in a CO_2 incubator (38.5°C, 5% O_2 and 5% CO_2). At 18 h after IVF, the fertilized oocytes were collected and removed to the embryonic culture medium as SOF medium supplemented with 4 mg/mL BSA, 1% nonessential amino acids (M7145, Sigma Aldrich, Shanghai, China), 2% essential amino acids (11,130,051, Thermo Fisher, Shanghai, China), 1 mM sodium pyruvate, 2 mM Gluta^{MAX}, 0.5 mM sodium citrate (T7461, Solarbio, Beijing, China) and 2.8 mM myo-inositol (I8050, Solarbio, Beijing, China) covered by mineral oil in a 35 mm sterile dish, followed by subsequent embryos' culture in a CO_2 incubator (38.5°C, 5% O_2 and 5% CO_2).

At 48 h after IVF, the presence of embryonic cleavage, as the successful symbol of fertilization, was microscopically examined by a stereomicroscope (745T, Nikon, Tokyo, China) with the embryonic cleavage rates of each group

calculated. Moreover, the embryos of each group were cultured for a subsequent 5 d with the culture medium changed every 48 h. At 7 d after IVF, the blastocyst development of each group was microscopically recorded with the blastocyst development rates calculated as the percentage of surviving embryos/fertilized oocytes.

Statistical Analysis

All experimental data in this study were presented as mean ± standard deviation (SD). The analyses of statistical data were conducted with the Statistical Package for the Social Sciences software (SPSS, IBM) with the statistical data among different groups analyzed by one-way ANOVA LSD tests. $p < 0.05$ was considered as significant in this study.

Results
The Characteristic Analysis of Se/CDs

The morphology of Se/CDs was analyzed by TEM with the results shown in Figure 1A. The TEM results revealed a typical monodisperse spherical nanosphere of Se/CDs, and the enlarged image shows a clear lattice structure of Se/CDs (Figure 1B). As shown in Figure 1C, the results of XPS demonstrated that the selenium had been successfully doped in CDs, and the doping ratio was 2.78%. The high-resolution XPS results and detailed element analysis were shown in Figure S1.

The deconvoluted C1s spectra in Figure S1A indicated the binding energy at 286.9 eV belongs to the C-N, C-O and C-Se. Furthermore, the peak at 288.3 eV and 284.7 eV attributed to C=O and C-C, C=C, respectively. The N1s spectrum in Figure S1B was fitted into the pyridinic N and NH_2 (399.5 eV) and cyano N (400.1 eV), meanwhile, the peak at 55.78 eV suggested the presence of C-Se-C (Figure S1C) and also proved the Se/CDs synthesized by our stepwise method.

To further certificate the components and surface state of the Se/CDs, the FT-IR spectra were obtained with the results shown in Figure 1D. The characteristic broad band from 3600 cm^{-1} to 3100 cm^{-1} should be associated with the N-H, O-H stretching vibration, and the small acromion at 2920 cm^{-1} attributed to the C-H stretching vibration. The strong
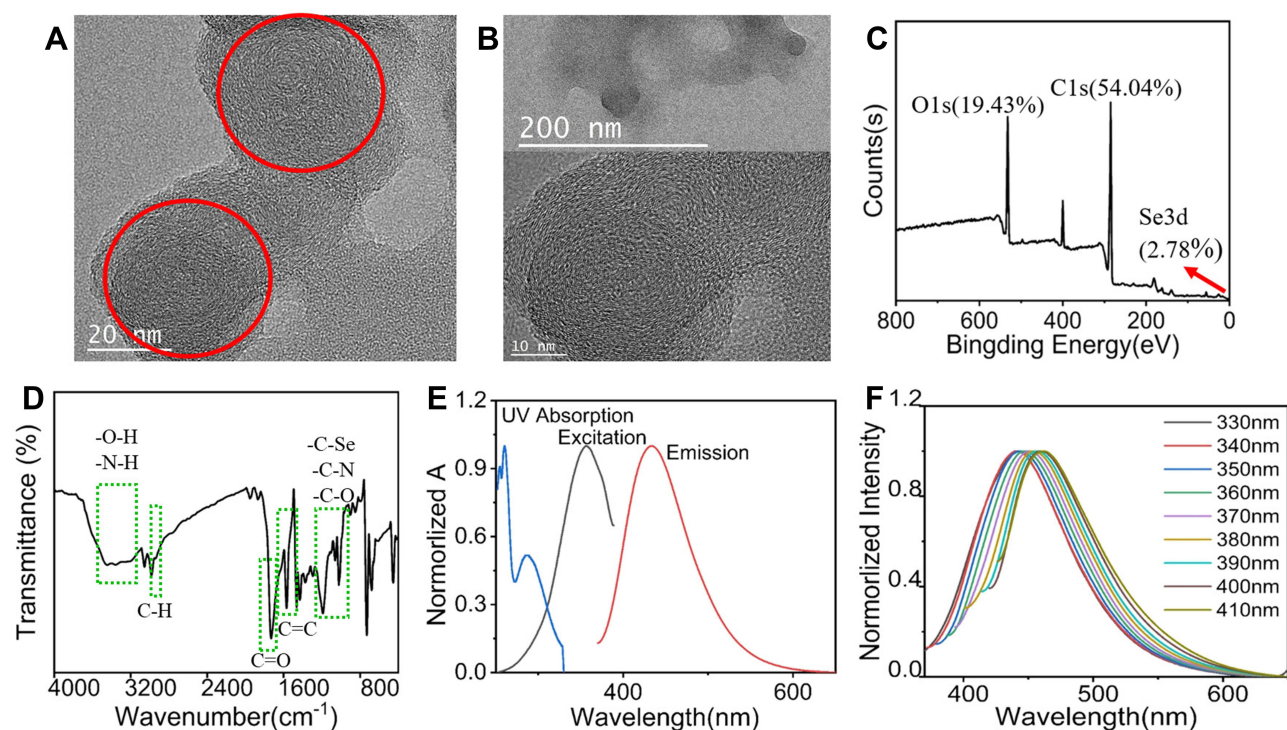

Figure 1 The characteristic f Se/CDs. (**A**) The TEM characteristic of Se/CDs. (**B**) The 200 nm, 10 nm morphology and lattice of Se/CDs. (**C**) XPS spectrum of Se-CDs. (**D**) The FT-IR spectrum scanning from 4000 cm-1 to 800 cm-1. (**E**) The UV absorption (blue), excitation (black), and emission (red) spectra of Se-CDs (λex =340 nm, λem = 360 nm). (**F**) The normalized excitation-dependent fluorescence emissions of Se/CDs (340–480 nm).
Notes: Scale bar= 20 nm. The red circles in the panel indicated the Se/CDs. The red arrows in the panel indicated Se 3d at 55.78 eV. The chemical bonds located in the Se/CDs were marked with the green dotted box.

absorption peak at 1727 cm^{-1} should be associated with the stretching vibration of C=O, while the 1580 cm^{-1}, 1552 cm^{-1} and 1430 cm^{-1} corresponded to the C=C stretching mode of aromatic domain. Band in the region from 1200–900 cm^{-1} referred to stretching vibration of C-Se, C-O and C-N. The results of FT-IR analysis, proving the abundant active functional groups on the surface of Se/CDs, were consistent with the XPS spectra, further confirming the water solubility of Se/CDs without more modification.

To evaluate the optical properties of Se/CDs, we determined the UV absorption spectrum, excitation and emission spectrum with the results shown in Figure 1E. The characteristic peaks in the ultraviolet region were observed, and two split peaks between 200–300 nm were assigned to the aromatic π orbitals electron transition of the nanocarbon structure. And the peak at 332 nm should be assigned to n-π* (C-Se, C-N or carboxyl) transitions on the surficial section of Se/CDs. Then we explored the luminescence properties of Se/CDs by the measurement of excitation and emission spectra with the results presented in Figure 1E. Under the excitation wavelength of 340 nm, the fluorescence emission probed from 200 to 600 nm, and the maximum was around 360 nm (the black line in Figure 1E). Then the emission wavelength was set as 360 nm, and the excitation spectrum of Se/CDs was tested with a maximum around 430 nm (the red line in Figure 1E). In order to determine the luminescence performance of Se/CDs, we measured the emission at different excitation wavelengths from 330 nm to 410 nm. As shown in Figure 1F, the Se/CDs synthesized in the present study possessed the obvious wavelength dependent characteristics as the excitation wavelength increased and the emission showed a significant red shift.

The Beneficial Effect of Se/CDs' Supplementation on the IVM Efficiency of Ovine Oocytes

The toxicity effects of Se/CDs' supplementation on the in vitro development competence of ovine oocytes and the potential effect of Se/CDs' supplementation on the IVM efficiency of ovine oocytes were analyzed with the results of oocyte survival rate and proliferation activity of cumulus cells presented in Figure S2, meanwhile, the oocyte maturation rates of each group were presented in Figure 2.

As shown in Figure S2A, there was no significant difference in the oocyte fragmentation rates among all experimental groups (p>0.05, 10.55±2.48% for NC group vs 11.50±2.24% for the LD group vs 10.51±1.57% for the MD group vs 9.92 ±2.35% for the HD group). Combined with the non-significant difference found in the proliferation potentials of cumulus cells among different groups (p>0.05, Figure S2B), these results confirmed the nontoxic effects of Se/CDs' supplementation on the in vitro development competence of ovine oocytes.

As shown in Figure 2, there was no obvious observation of cellular damage in the COCs after IVM and MII oocytes after Se/CDs' supplementation, regardless of the increasing concentration of Se/CDs' supplementation. Moreover, the maturation rates of MD (82.84±5.21%) and HD (84.71±4.99%) groups were significantly higher than that of the NC group (68.08±5.07%)(p<0.05). Although there was non-significant difference in the maturation rates between the NC and LD (72.97±4.05%) groups (p>0.05), these results at least confirmed the nonexistence of toxicity effect of Se/CDs and the beneficial effect of 100 μg/mL and 200 μg/mL Se/CDs' supplementation on the IVM efficiency of ovine oocytes.

The Beneficial Effect of Se/CDs' Supplementation on the Cytoplasmic Maturation and Mitochondrial Activities of Ovine MII Oocytes

As the symbol of cytoplasmic maturation after IVM, CGs' dynamics of ovine MII oocytes were investigated with the representative results of LCA-FITC staining shown in Figure 3.

As indicated in Figure 3A and D, the results of LCA-FITC staining confirmed that the positive signals of CGs were mainly located in the subcortical region of ovine MII oocytes, consistent with our former study.[3,17] In addition, the positive staining intensities of CGs' signals in the MD and HD groups were significantly up-regulated compared with these of NC and LD groups (p<0.05). The significant increase in the CGs' signals from the NC group to LD group (p<0.05) further revealed that the Se/CDs' supplementation effectively promoted the cytoplasmic maturation of ovine MII oocytes.
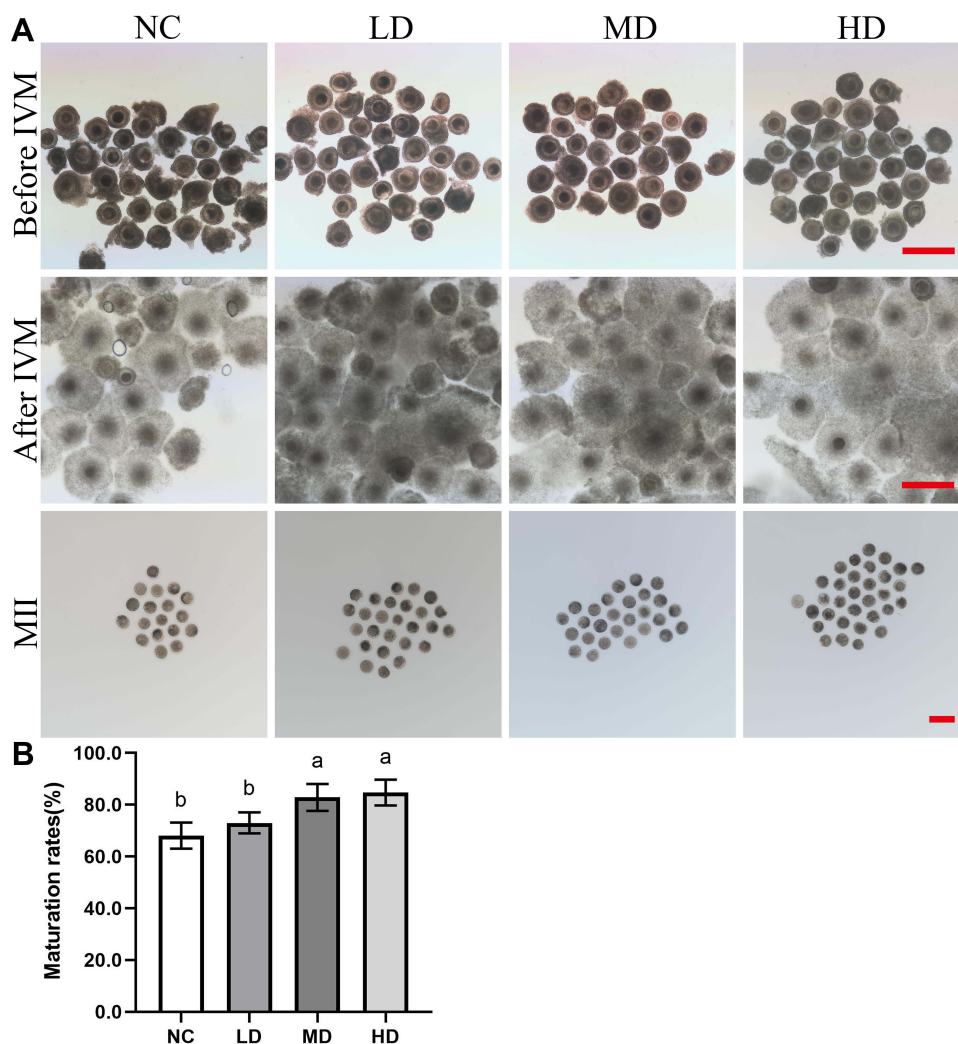
Figure 2 The effect of Se/CDs' supplementation on the IVM efficiency of ovine oocytes. (**A**) Morphology of COCs before IVM, COCs after IVM and MII oocytes. (**B**) Maturation rates.

Notes: NC represents the negative control group. LD, MD and HD represent the Se/CDs groups supplemented with 50, 100 and 200 μg/mL of Se/CDs, respectively. The red scale bar of COCs before IVM=500 μm. The red scale bar of COCs after IVM=500 μm. The red scale bar of MII oocytes=100 μm. NC represents the negative control group. LD, MD and HD represent the Se/CDs groups supplemented with 50, 100 and 200 μg/mL of Se/CDs, respectively. The different lowercase letters in each column indicate significant differences between different groups (p<0.05).

In addition, the mitochondrial activities in ovine MII oocytes after Se/CDs' supplementation were also analyzed by the assay of mitochondrial activity and ROS production level with the representative staining results of MitoTracker staining and DCFH-DA staining presented in Figure 3.

As indicated in Figure 3B and E, the results of MitoTracker staining showed that the positive signals of MitoTracker in the LD, MD, and HD groups were significantly up-regulated in comparison with that of the NC group (p<0.05). In addition, the significant increase of MitoTracker signals among all Se/CDs groups in a dose dependent manner suggested the promising effect of Se/CDs' supplementation on the mitochondrial activities of ovine MII oocytes.

Meanwhile, the DCFH-DA staining intensities in the LD, MD, and HD groups were significantly lower than that of the NC group (Figure 3C and F, p<0.05). Moreover, the decreased DCFH-DA staining intensities in ovine MII oocytes were positively related to the increased concentrations of Se/CDs supplementation (p<0.05).

These results, combined with the results of oocyte maturation and CGs' dynamics, confirmed the beneficial effects of Se/CDs' supplementation on the maturation of ovine MII oocytes via promoting mitochondrial activities.
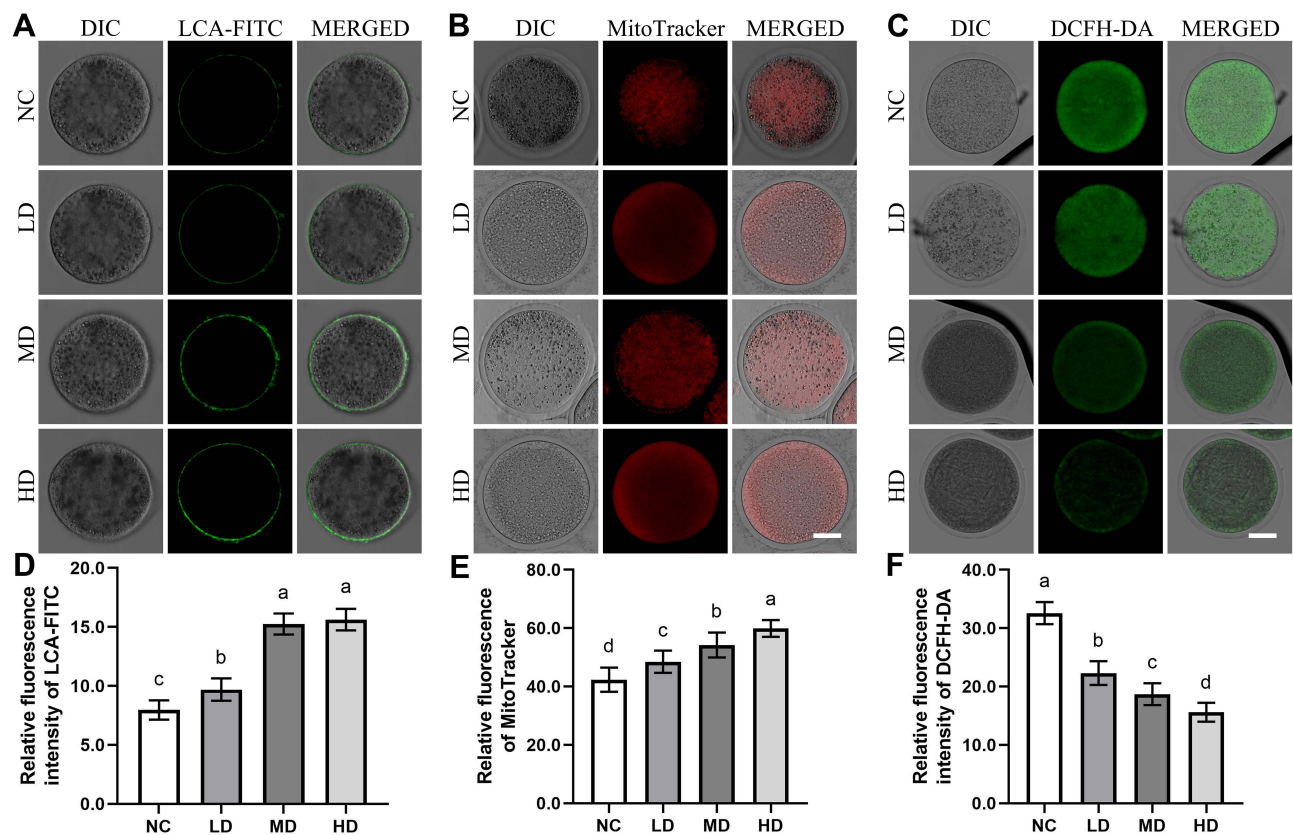
Figure 3 The effect of Se/CDs' supplementation on the cytoplasmic maturation, mitochondrial activities and ROS production levels of ovine MII oocytes.
Notes: (**A**) CGs' dynamics staining of ovine MII oocytes. (**B**) MitoTracker staining of ovine MII oocytes. NC represents the negative control group. LD, MD and HD represent the Se/CDs groups supplemented with 50, 100 and 200 μg/mL of Se/CDs, respectively. LCA-FITC represents the LCA-FITC staining specific for the CGs dynamics of ovine MII oocytes. DIC, differential interference contrast microscope, represents the bright field of ovine MII oocytes after LCA-FITC staining. MERGED represents the merged results of LCA-FITC staining and bright field. Scale bar=50 μm. NC represents the negative control group. LD, MD and HD represent the Se/CDs groups supplemented with 50, 100 and 200 μg/mL of Se/CDs, respectively. MitoTracker represents the MitoTracker staining of different groups. DIC represents the bright field of ovine MII oocytes after MitoTracker staining. MERGED represents the merged results of MitoTracker staining and DIC. Scale bar=50 μm. (**C**) DCFH-DA staining of ovine MII oocytes. (**D**) Relative fluorescence intensity of LCA-FITC. NC represents the negative control group. LD, MD and HD represent the Se/CDs groups supplemented with 50, 100 and 200 μg/mL of Se/CDs, respectively. DCFH-DA represents the DCFH-DA staining of different groups. DIC represents the bright field of ovine MII oocytes after DCFH-DA staining. MERGED represents the merged results of DCFH-DA staining and DIC. Scale bar=50 μm. (**E**) Relative fluorescence intensity of MitoTracker. (**F**) Relative fluorescence intensity of DCFH-DA NC represents the negative control group. LD, MD and HD represent the Se/CDs groups supplemented with 50, 100 and 200 μg/mL of Se/CDs, respectively. The different lowercase letters in each column indicate significant differences between different groups ($p<0.05$).

The Beneficial Effect of Se/CDs' Supplementation on the Epigenetic Modifications of Ovine MII Oocytes

Due to the key roles of epigenetic modifications during mammalian oocyte maturation and fertilization, the epigenetic modifications including histone modifications (H3K9me3 and H3K27me3) and DNA modifications (5mC and 5hmC) of ovine MII oocytes induced by the Se/CDs' supplementation were investigated by immunofluorescence staining with the representative staining results shown in Figures 4 and 5.

As indicated in Figure 4, the expression levels of H3K9me3 and H3K27me3 in all Se/CDs treatment groups were remarkably enhanced in comparison with those of the NC groups ($p<0.05$), indicating the enhanced histone methylation levels in ovine MII oocytes after Se/CDs' supplementation. Although the expression levels of H3K9me3 and H3K27me3 in the LD group were statistically lower in comparison with those of the MD and HD groups, there was no significant difference in the expression levels of H3K9me3 and H3K27me3 between the MD and HD groups ($p>0.05$).

In addition, the 5mC and 5hmC staining results, present in Figure 5, confirmed that the expression patterns of 5mC and 5hmC in the HD and MD groups were effectively enhanced compared with those of the NC and LD groups ($p<0.05$). Moreover, the positive relationships between the increased fluorescence intensities of 5mC and 5hmC staining and
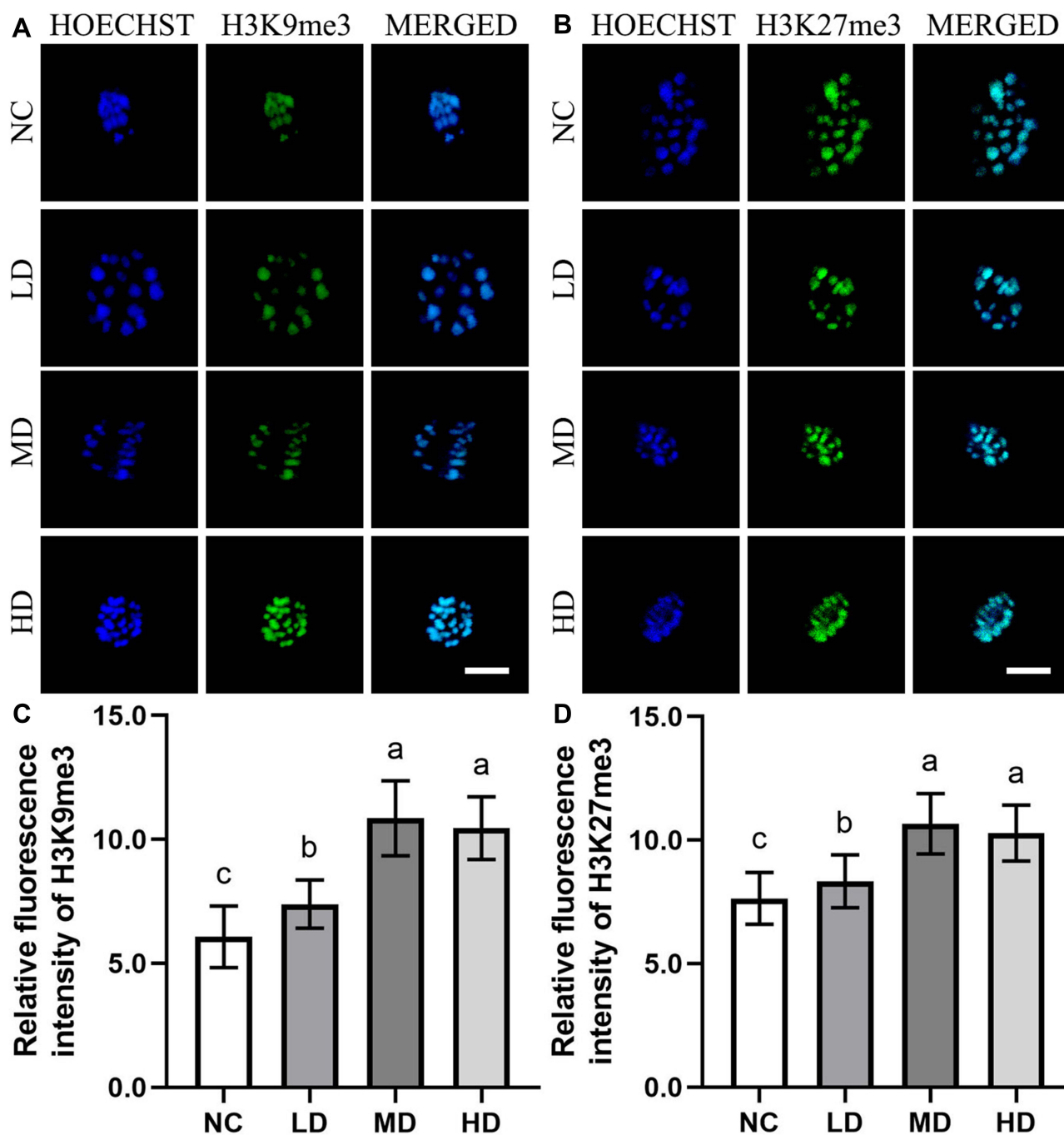
Figure 4 The effect of Se/CDs' supplementation on the histone methylation levels of ovine MII oocytes. (**A**) H3K9me3 immunofluorescence staining of ovine MII oocytes. (**B**) H3K27me3 immunofluorescence staining of ovine MII oocytes. (**C**) Relative fluorescence intensity of H3K9me3. (**D**) Relative fluorescence intensity of H3K27me3.
Notes: NC represents the negative control group. LD, MD and HD represent the Se/CDs groups supplemented with 50, 100 and 200 μg/mL of Se/CDs, respectively. HOECHST represents the Hoechst 33,342 staining of different groups. H3K9me3 represents the H3K9me3 immunofluorescence staining of different groups. MERGED represents the merged results of H3K9me3 staining and Hoechst 33,342 staining. Scale bar=5 μm. NC represents the negative control group. LD, MD and HD represent the Se/CDs groups supplemented with 50, 100 and 200 μg/mL of Se/CDs, respectively. HOECHST represents the Hoechst 33,342 staining of different groups. H3K27me3 represents the H3K27me3 immunofluorescence staining of different groups. MERGED represents the merged results of H3K27me3 staining and Hoechst 33,342 staining. The scale bar=5 μm. NC represents the negative control group. LD, MD and HD represent the Se/CDs groups supplemented with 50, 100 and 200 μg/mL of Se/CDs, respectively. The different lowercase letters in each column indicate significant differences between different groups (p<0.05). NC represents the negative control group. LD, MD and HD represent the Se/CDs groups supplemented with 50, 100 and 200 μg/mL of Se/CDs, respectively. The different lowercase letters in each column indicate significant differences between different groups (p<0.05).
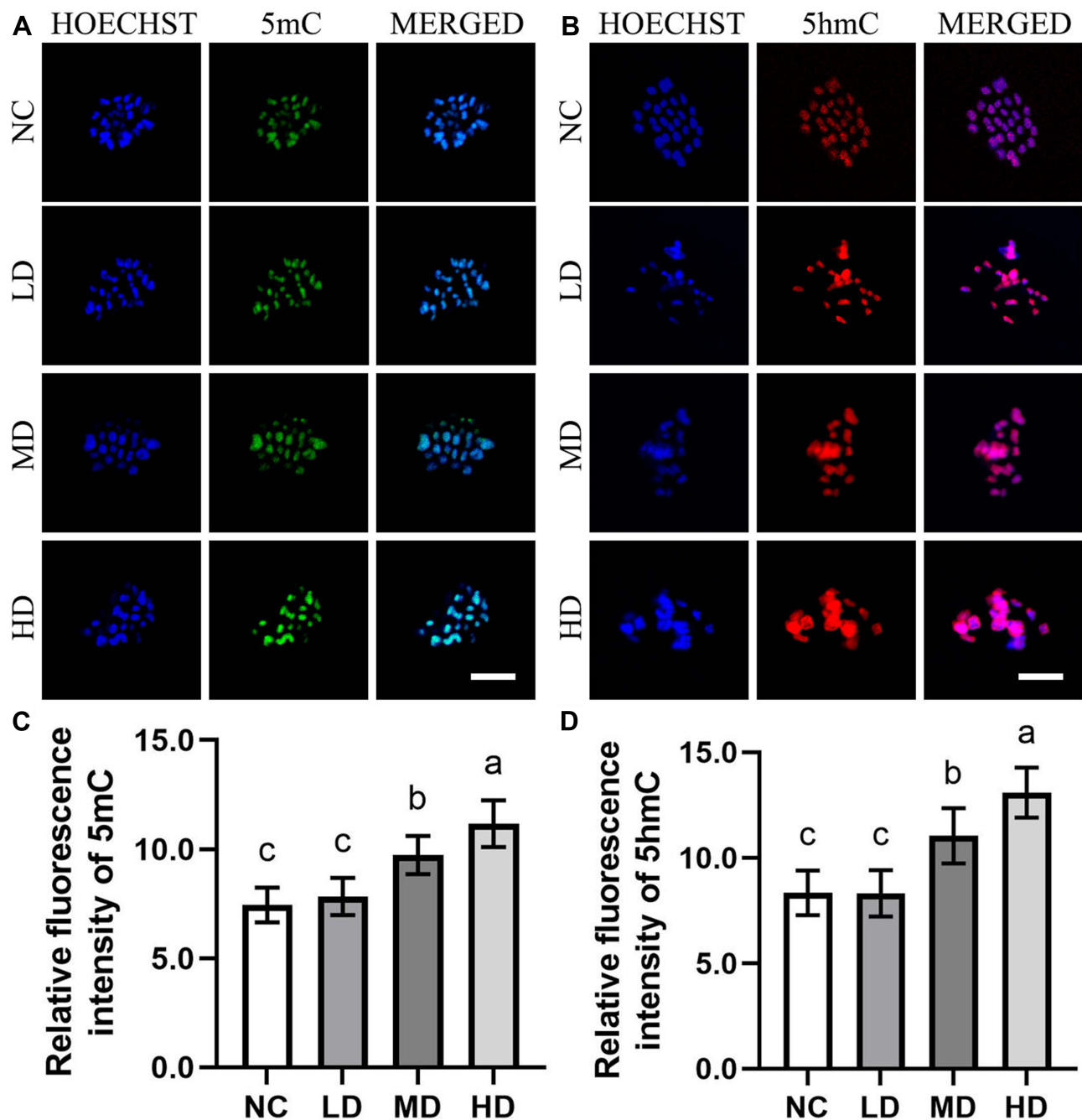
Figure 5 The effect of Se/CDs' supplementation on the DNA methylation levels of ovine MII oocytes. (**A**) 5mC immunofluorescence staining of ovine MII oocytes. (**B**) 5hmC immunofluorescence staining of ovine MII oocytes. (**C**) Relative fluorescence intensity of 5mC. (**D**) Relative fluorescence intensity of 5hmC.

Notes: NC represents the negative control group. LD, MD and HD represent the Se/CDs groups supplemented with 50, 100 and 200 μg/mL of Se/CDs, respectively. HOECHST represents the Hoechst 33,342 staining of different groups. 5mC represents the 5mC immunofluorescence staining of different groups. MERGED represents the merged results of 5mC staining and Hoechst 33,342 staining. Scale bar=5 μm. NC represents the negative control group. LD, MD and HD represent the Se/CDs groups supplemented with 50, 100 and 200 μg/mL of Se/CDs, respectively. HOECHST represents the Hoechst 33,342 staining of different groups. 5hmC represents the 5hmC immunofluorescence staining of different groups. MERGED represents the merged results of 5hmC staining and Hoechst 33,342 staining. Scale bar=5 μm. NC represents the negative control group. LD, MD and HD represent the Se/CDs groups supplemented with 50, 100 and 200 μg/mL of Se/CDs, respectively. The different lowercase letters in each column indicate significant differences between different groups (p<0.05). NC represents the negative control group. LD, MD and HD represent the Se/CDs groups supplemented with 50, 100 and 200 μg/mL of Se/CDs, respectively. The different lowercase letters in each column indicate significant differences between different groups (p<0.05).

increased Se/CDs concentrations (p<0.05) revealed the promising effect of Se/CDs' supplementation on the histone and DNA methylation patterns of ovine MII oocytes.

The Potential Effect of Se/CDs' Supplementation on the Fertilization Potentials of Ovine MII Oocytes

To confirm the potential effect of Se/CDs' supplementation on the development competence of ovine MII oocytes, fertilization potential assays including fertilization rates and embryonic developmental abilities of ovine MII oocytes were conducted with the results presented in Figure 6.

As shown in Figure 6A and B, the fertilization assay showed that the Se/CDs' supplementation effectively promoted the fertilization potentials of ovine MII oocytes with the fertilization rates effectively up-regulated from 63.00±8.01% for the NC group, 80.13±6.09% for the MD group to 81.99±8.42% for the HD group (p<0.05), regardless of the non-significant difference in the fertilization rates between the NC and LD groups (64.20±7.71%) (p>0.05). In addition, there was non-significant difference in the fertilization rates between the MD and HD groups (p>0.05).

Meanwhile, the blastocyst developmental assay (Figure 6C) confirmed the beneficial effect of Se/CDs' supplementation on the fertilization potentials of ovine MII oocytes, as the blastocyst developmental rates of ovine MII oocytes were remarkably up-regulated from 24.58±5.84% for NC group, 28.08±2.75% for LD group to 37.44±3.33% for MD group and 40.35±2.18% for the HD group (p<0.05). Consistent with the fertilization results, there was non-significant difference in the blastocyst developmental rates between the MD and HD groups (p>0.05).

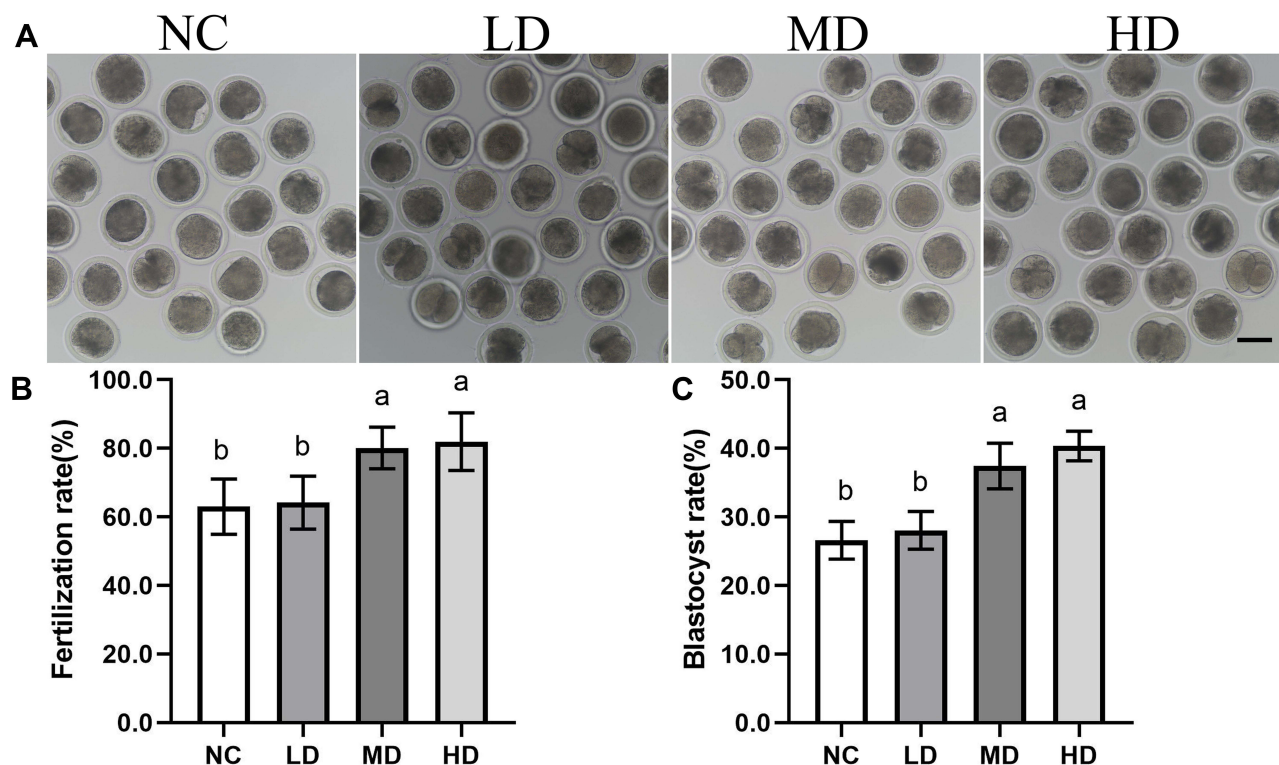**Figure 6** The effect of Se/CDs' supplementation on the embryonic development potentials of ovine MII oocytes. (**A**) Morphology of 2-cells after IVF. (**B**) Fertilization rates. (**C**) Blastocyst development rates.
Notes: NC represents the negative control group. LD, MD and HD represent the Se/CDs groups supplemented with 50, 100 and 200 μg/mL of Se/CDs, respectively. Scale bar =100 μm. NC represents the negative control group. LD, MD and HD represent the Se/CDs groups supplemented with 50, 100 and 200 μg/mL of Se/CDs, respectively. The different lowercase letters in each column indicate significant differences between different groups (p<0.05). NC represents the negative control group. LD, MD and HD represent the Se/CDs groups supplemented with 50, 100 and 200 μg/mL of Se/CDs, respectively. The different lowercase letters in each column indicate significant differences between different groups (p<0.05).

The Potential Effect of Se/CDs' Supplementation on the Transcript Profiles of Ovine MII Oocytes

According to these results, the transcript profiles of ovine MII oocytes of the NC and MD groups were analyzed by Smart-Seq to finally confirm the potential effect of Se/CDs' supplementation on the transcriptional profiles of ovine MII oocytes.

As shown in Figure 7A and B, the transcript profiles of MD group were significantly different from those of the NC group as 846 transcripts were effectively repressed and 2994 transcripts were remarkably up-regulated in the MD group in comparison with those of the NC group. In particular, the KEGG enrichment analysis revealed that DEGs between the NC and MD groups were enriched in the mitochondrial oxidative phosphorylation and oocyte meiosis pathways (Figure 7C and D).

Consistent with the enhanced maturation rates of ovine oocytes after the Se/CDs' supplementation, the up-regulated expression levels of oocyte maturation related genes including *BMP15, SF1, STC1, WEKK2, MAPK1, CDC25C, PLK1, MAP2K1, AURKA, SIRT2, SIRT3, SIRT5* and *SIRT7* in the MD group (Figure 7E) further confirmed the beneficial effect of Se/CDs' supplementation on the oocyte maturation (absolute fold change≥2). Moreover, the Se/CDs' supplementations effectively promoted the expression levels of *NRF1, GPX1, BRCA1, MTCH2* and *ARAF1* (Figure 7E), further revealing the beneficial effect of Se/CDs' supplementation on the mitochondrial activity of ovine oocytes. In addition, the enhanced expression levels of epigenetic medication related genes such as *TET1, TET2, TET3, KDM5B, KDM4B, HIFOO* and *HDAC3* also confirmed the promising effect of Se/CDs' supplementation on the epigenetic medication of ovine oocytes.
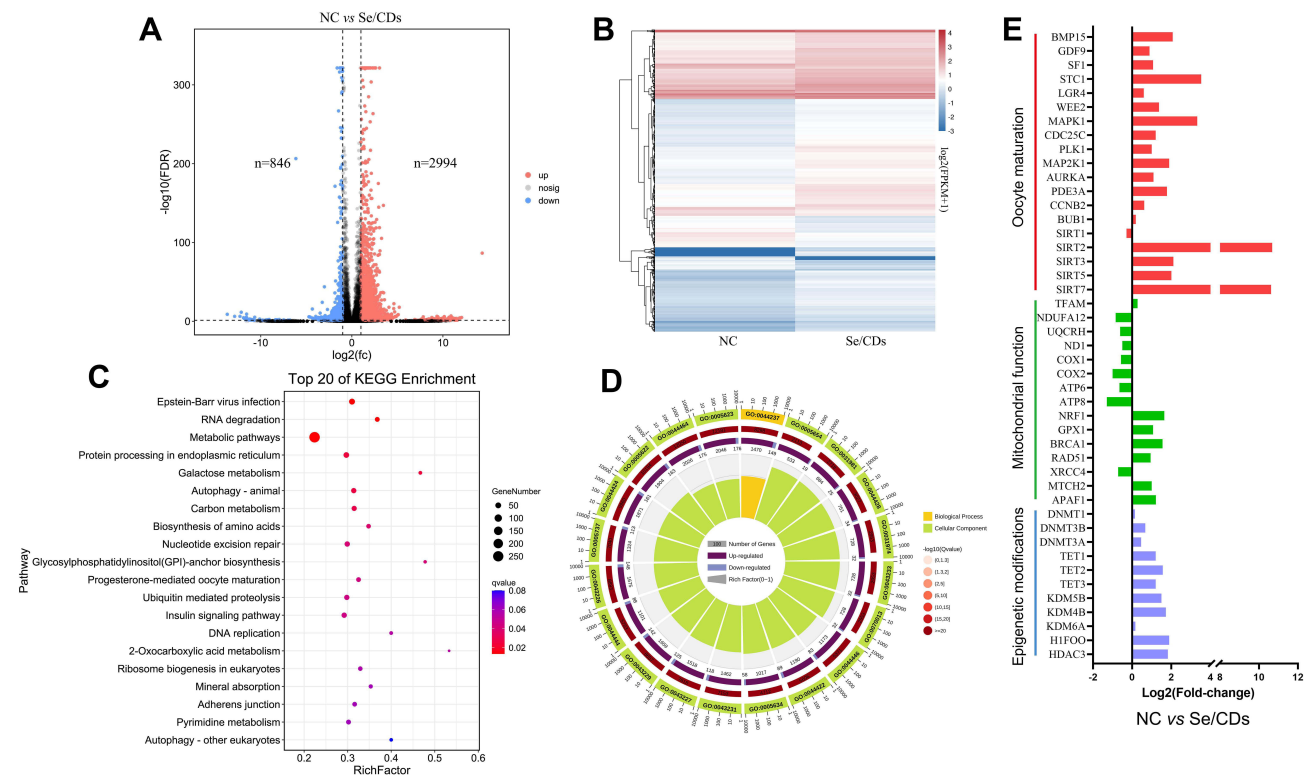

Figure 7 The effect of Se/CDs' supplementation on the transcript profiles of ovine MII oocytes. (**A**) Numbers of differentially expressed genes (DEGs) that are abnormally repressed (blue) or upregulated (red) in the Se/CDs group compared to the NC group. (**B**) Heatmap illustration showing the DEGs in the Se/CDs group compared to the NC group. (**C**) Top 20 KEGG pathways enriched in the Se/CDs group compared to the NC group. (**D**) GO analyses of the DEGs in the Se/CDs group compared to the NC group. (**E**) Expression levels of DEGs related to oocyte maturation, mitochondrial functions and epigenetic modifications in the NC and Se/CDs groups.
Notes: NC represents the negative control group. Se/CDs represent the Se/CDs group supplemented with 100 μg/mL of Se/CDs, respectively.

Discussion

As organelles with biomembrane structures, mitochondria integrate with the complex pathways related to cellular metabolic, redox and calcium signaling to maintain the metabolism, redox homeostasis, and fatty acid oxidation in mammalian cells.[33] The Se deficiency reduces the synthesis of intracellular glutathione (GSH) in mammalian cells,[34] further triggering the mitochondrial dysfunctions. The mitochondrial dysfunctions caused by the Se deficiency subsequently cause the abnormal accumulation of ROS and elevated oxidative stress, resulting in complex diseases including renal dysfunction,[35] heart failure,[36] intestinal damage[37] and thyroid disorders.[38] Moreover, maternal Se deficiencies alter the fetal development and predispose the adult offspring to thyroid dysfunction and fetal growth restriction via the alterations of mitochondrial protein expression.[39]

Due to the key effect of mitochondrial dysfunctions induced by Se deficiencies on disease progression, the supplementation of antioxidant compounds including sodium selenite (Na_2SeO_3), sodium selenate (Na_2SeO_4) and Se enriched yeast (SY) has been applied to ameliorate the oxidative stress damage caused by the exposure of bisphenol A (BPA),[40] doxorubicin,[41] monosodium glutamate,[42] aluminum,[43] docetaxel (DTX),[44] sodium azide (SA)[45] and aflatoxin B1 (AFB1)[46] via the promotion of mitochondrial functions. Furthermore, the artificial selenylation modifications of polymannuronate, polysaccharides and galactomannan (GM) have been confirmed to promote neuroprotection,[47,48] anti-inflammatory,[49,50] anti-tumor activity,[51,52] hepatic protection[53,54] and antiglycative activity[55] of these biopolymers via the promotion of antioxidant defense system. Moreover, the Se/CDs have been confirmed to have the capability for free radicals scavenging,[56,57] facilitating the promotion of antioxidant defense system. However, the potential effects of Se/CDs' supplementation on the development competences of mammalian oocytes have been rarely reported.

According to the enhanced potentials of maturation rates, CGs' dynamics, mitochondrial activities and fertilization capacities combined with the decreased ROS production levels in ovine MII oocytes after Se/CDs' supplementation, our study firstly confirmed that the supplementation of Se/CDs, synthesized by the facile hydrothermal treatment of DPDSe, remarkably enhanced the developmental potentials of ovine MII oocytes. Moreover, the results of Smart-Seq assay confirmed the beneficial effect of Se/CDs' supplementation on ovine oocytes, evidenced by the up-regulated expression levels of *BMP15, SF1, STC1, WEKK2, MAPK1, CDC25C, PLK1, MAP2K1, AURKA, SIRT2, SIRT3, SIRT5* and *SIRT7* in the Se/CDs supplementation group. Meanwhile, the up-regulated expression levels of *NRF1, GPX1, BRCA1, MTCH2* and *ARAF1*, in combination with the MitoTracker staining results, further confirmed the positive corrections between the Se/CDs' supplementation and ovine oocyte development via the promotion of mitochondrial functions.

During the facile hydrothermal synthesis of Se/CDs, these seleno amino acids including selenomethionine and selenocystine were the traditional precursors.[56,57] However, Li et al found that during the synthesis Se/CDs with selenocystine as precursor, Se disappeared from the Se/CDs when the reaction temperature was above 90°C.[56] Due to the key role of higher temperature in the better formation of stable CQDs,[58] DPDSe was firstly used as the precursor for the synthesis of Se/CDs at 200°C, overcoming the dependence of seleno amino acids in the process of Se/CDs' synthesis. DPDSe, as a simple synthetic organoselenium compound and a glutathione peroxidase (GPx) enzyme mimic, has been recognized as a promising pharmacological agent with specific properties including anticancer, anti-inflammatory, antidiabetic, antioxidant and neuroprotection even with relatively low doses.[59] During the regulation of antioxidant defense system, DPDSe not only reduces the accumulation levels of ROS, but prevents the oxidative damage to lipids, proteins and DNA via promoting the expression levels of antioxidant related genes.[60] In consistent with these former publications with the antioxidant effect of DPDSe, the significant increases of mitochondrial activities and decreased ROS production levels were found in ovine oocytes after Se/CDs' supplementation, introducing a new and cheap alternative for the synthesis of Se/CDs with DPDSe as precursor.

Considering the key role of cumulus cells during the process of in vivo oogenesis and in vitro oocyte maturation, the non-significant differences in the proliferation potentials of cumulus cells and oocyte survival rate between the NC and Se/CDs supplementation groups further confirmed the biosafety of Se/CDs synthesized with DPDSe as precursor. In contrast, Hsieh et al found that the exposure of CdSe/CDs altered the murine oocyte maturation, fertilization, and in vitro embryo development potentials,[61] in consistent with the results of Xu's study.[62] We presumed the different results in the outcomes of murine and ovine oocyte development between the Se/CDs' supplementation and other CDs' exposure were

mainly due to the different physicochemical properties of core materials doped with CDs. Although the in vitro cytotoxicity induced by CDs has been reported with the potentials of dose-, shape-, size-, surface chemistry-, surface charge- and cell type-dependent manner, it does not solely depend on a single factor but rather depends on a complex combination of several factors.[63] More detailed investigations should be conducted to confirm the biosafety effect of Se/CDs' supplementation on the mammalian IVM and breeding technology.

Moreover, the enhanced staining intensities in the histone methylation of H3K9me3 and H3K27me3 and DNA methylation of 5mC and 5hmC in the Se/CDs groups compared with that of the NC group were also found in the present study, revealing the significantly enhanced histone and DNA methylation process in ovine oocyte after the Se/CDs' supplementation. Meanwhile, the enhanced histone and DNA methylation levels in ovine oocytes after the Se/CDs' supplementation were also confirmed by the up-regulated expression levels of epigenetic medication related genes such as *TET1, TET2, TET3, KDM5B, KDM4B, HIFOO* and *HDAC3*.

The epigenetic modifications of histone and DNA methylation play important roles in the regulation of oocyte development and the following fertilization potentials. The epigenetic alterations induced by advanced maternal aging, mitochondrial dysfunctions, abnormal nutrition supply and abnormal expression levels of hormones trigger seriously meiotic defects of mammalian gametes, subsequently resulting in the incidence of aneuploidy after fertilization and embryonic development defects.[17] In consistent with our present study, these former literature have revealed that the promotion of epigenetic modifications via the amelioration of mitochondrial dysfunctions significantly improved the development potentials of mammalian oocytes,[16,17,64–66] further addressing the future applications of Se/CDs as dietary supplementation in mammalian IVM via the promotion of epigenetic modifications. However, the specific regulation mechanism related to the effect of Se/CDs' supplementation in the epigenetic modifications of ovine MII oocytes and the potential effect of Se/CDs' supplementation on the epigenetic modifications of ovine zygote and/or blastocyst need more detailed investigations.

Conclusion

Taken together, these results investigated the potential application and regulation related mechanism of Se/CDs' supplementation in the IVM of ovine oocytes. And we hope that the enhanced development potentials and transcript profiles of ovine MII oocytes after Se/CDs' supplementation will benefit future research about the clinical applications of Se/CDs and the improvements in ART for ovine breeding.

Abbreviations

Se/CDs, selenium doped carbon quantum dots; CGs, cortical granules; ROS, reactive oxygen species; IVM, in vitro maturation; DEGs, differentially expressed genes; GO, Gene Ontology; KEGG, Kyoto Encyclopedia of Genes and Genomes; IVF, in vitro fertilization; ET, embryo transfer; IVP, in vitro production; OPU, ovum pick-up; ATP, adenosine triphosphate; 5mC, 5-methylcytosine; H3K9me3, H3, lysine 9 trimethylation; SeNPs, selenium nano-particles; ZnNPs, zinc nano-particles; CDs, carbon quantum dots; Se, selenium; TEM, transmission electron microscopy; XRD, X-ray diffraction; XPS, X-ray Photoelectron Spectroscopy; PL, photoluminescence; FT-IR, Fourier transform infrared; COCs, cumulus oocyte complexes; BSA, bovine serum albumin; EGF, epidermal growth factor; FBS, fetal bovine serum; FSH, follicle stimulating hormone; LH, luteinizing hormone; H-SOF, Hepes-synthetical oviductal fluid; PBE, polar body extrusion; MII, metaphase II; PFA, paraformaldehyde solution; DPBS, Dulbecco's phosphate buffered saline; DCFH-DA, dichlorofluorescein diacetate solution; rRNA, Ribosome RNA; FPKM, fragment per kilobase of transcript per million mapped reads; FDR, false discovery rate; SD, standard deviation; SPSS, Statistical Package for the Social Sciences software; BPA, bisphenol A; DTX, docetaxel; SA, sodium azide; AFB1, aflatoxin B1; PCD, programmed cell death; SIRT1, sirtuin 1; SIRT2, sirtuin 2; SIRT3, sirtuin 3; SF1, splicing factor 1; BMP15, bone morphogenetic protein 15; STC1, stanniocalcin 1; GDF9, growth differentiation factor 9; SIRT5, sirtuin 5; WEE2, WEE1 homolog 2; BUB1, BUB1 mitotic checkpoint serine/threonine kinase; LGR4, leucine rich repeat containing G protein-coupled receptor 4; MAPK1, mitogen-activated protein kinase 1; CDC25C, cell division cycle 25C; PLK1, polo like kinase 1; SIRT7, sirtuin 7; MAP2K1, mitogen-activated protein kinase kinase 1; AURKA, aurora kinase A; PDE3A, phosphodiesterase 3A; CCNB2, cyclin B2; PDE3A, cGMP-inhibited 3',5'-cyclic phosphodiesterase A; BUB1, mitotic checkpoint serine/

threonine-protein kinase BUB1; ND1, NADH dehydrogenase subunit 1; COX1, cytochrome c oxidase subunit I; COX2, cytochrome c oxidase subunit II; ATP8, ATP synthase F0 subunit 8; ATP6, ATP synthase F0 subunit 6; TFAM, transcription factor A, mitochondrial; NRF1, nuclear respiratory factor 1; BRCA1, BRCA1, DNA repair associated; MTCH2, mitochondrial carrier 2; APAF1, apoptotic peptidase activating factor 1; XRCC4, X-ray repair cross comple-menting 4; NDUFA12, NADH, ubiquinone oxidoreductase subunit A12; RAD51, RAD51 recombinase; UQCRH, cytochrome b-c1 complex subunit 6, mitochondrial; GPX1, glutathione peroxidase 1; HDAC3, histone deacetylase 3; KDM6A, lysine demethylase 6A; DNMT3B, microtubule associated protein RP/EB family member 1; TET1, tet methylcytosine dioxygenase 1; KDM4B, lysine demethylase 4B; TET2, tet methylcytosine dioxygenase 2; TET3, tet methylcytosine dioxygenase 3; H1FOO, histone H1oo; DNMT1, DNA methyltransferase 1; DNMT3A, DNA methyl-transferase 3 alpha; KDM5B, lysine-specific demethylase 5B.

Data Sharing Statement

We declared that materials described in the manuscript, including all relevant raw data, will be freely available to any scientist wishing to use them for non-commercial purposes, without breaching participant confidentiality.

Ethics Approval and Consent to Participate

During the process of animal-related experiments, all the protocols were approved by the Ethics Committee of Inner Mongolia Medical University and conducted under the welfare management of Experimental Animals of Inner Mongolia Medical University.

Acknowledgment

Funding

Disclosure

The authors report no conflicts of interest in this work.

References

1. Heape W. Preliminary note on the transplantation and growth of mammalian ova within a uterine foster-mother. *Proc R Soc Lond*. 1890;48:457–458. doi:10.1098/rspl.1890.0053
2. Hansen PJ. Current and future assisted reproductive technologies for mammalian farm animals. *Adv Exp Med Biol*. 2014;752. doi:10.1007/978-1-4614-8887-3_1
3. Ren J, Hao Y, Liu Z, et al. Effect of exogenous glutathione supplementation on the in vitro developmental competence of ovine oocytes. *Theriogenology*. 2021;173:144–155. doi:10.1016/j.theriogenology.2021.07.025
4. Li S, Liu M, Ma H, et al. Ameliorative effect of recombinant human lactoferrin on the premature ovarian failure in rats after cyclophosphamide treatments. *J Ovarian Res*. 2021;14(1):17. doi:10.1186/s13048-020-00763-z
5. Duffy DM, Ko C, Jo M, Brannstrom M, Curry TE. Ovulation: parallels With Inflammatory Processes. *Endocr Rev*. 2019;40(2):369–416. doi:10.1210/er.2018-00075
6. Cheng XT, Sheng ZH. Developmental regulation of microtubule-based trafficking and anchoring of axonal mitochondria in health and diseases. *Dev Neurobiol*. 2020;81:284–299. doi:10.1002/dneu.22748
7. Cobley JN. Mechanisms of mitochondrial ROS production in assisted reproduction: the known, the unknown, and the intriguing. *Antioxidants*. 2020;9(10):933. doi:10.3390/antiox9100933
8. Malott KF, Luderer U. Toxicant effects on mammalian oocyte mitochondria. *Biol Reprod*. 2021;104:784–793. doi:10.1093/biolre/ioab002
9. Azzam EI, Jay-Gerin JP, Pain D. Ionizing radiation-induced metabolic oxidative stress and prolonged cell injury. *Cancer Lett*. 2012;327(1–2):48–60. doi:10.1016/j.canlet.2011.12.012
10. Salnikow K, Zhitkovich A. Genetic and epigenetic mechanisms in metal carcinogenesis and cocarcinogenesis: nickel, arsenic, and chromium. *Chem Res Toxicol*. 2008;21(1):28–44. doi:10.1021/tx700198a

11. Kalo D, Roth Z. Effects of mono (2-ethylhexyl) phthalate on cytoplasmic maturation of oocytes–The bovine model. *Reprod Toxicol*. 2015;53:141–151. doi:10.1016/j.reprotox.2015.04.007

12. Zhang JW, Xu DQ, Feng XZ. The toxic effects and possible mechanisms of glyphosate on mouse oocytes. *Chemosphere*. 2019;237:124435. doi:10.1016/j.chemosphere.2019.124435

13. Chiaratti MR, Garcia B, Carvalho K, et al. Oocyte mitochondria: role on fertility and disease transmission. *Anim Reprod*. 2018;15:231–238. doi:10.21451/1984-3143-AR2018-0069

14. Cheng Y, Zhang J, Wu T, et al. Reproductive toxicity of acute Cd exposure in mouse: resulting in oocyte defects and decreased female fertility. *Toxicol Appl Pharmacol*. 2019;379:114684. doi:10.1016/j.taap.2019.114684

15. Fan LH, Wang ZB, Li QN, et al. Absence of mitochondrial DNA methylation in mouse oocyte maturation, aging and early embryo development. *Biochem Biophys Res Commun*. 2019;513(4):912–918. doi:10.1016/j.bbrc.2019.04.100

16. Zhang X, Zhou C, Li W, et al. Vitamin C protects porcine oocytes from microcystin-lr toxicity during maturation. *Front Cell Dev Biol*. 2020;8:582715. doi:10.3389/fcell.2020.582715

17. Ren J, Li S, Wang C, et al. Glutathione protects against the meiotic defects of ovine oocytes induced by arsenic exposure via the inhibition of mitochondrial dysfunctions. *Ecotoxicol Environ Saf*. 2021;230:113135. doi:10.1016/j.ecoenv.2021.113135

18. May-Panloup P, Boucret L, Chao de la Barca JM, et al. Ovarian ageing: the role of mitochondria in oocytes and follicles. *Hum Reprod Update*. 2016;22(6):725–743. doi:10.1093/humupd/dmw028

19. Labarta E, de Los Santos MJ, Escribá MJ, Pellicer A, Herraiz S. Mitochondria as a tool for oocyte rejuvenation. *Fertil Steril*. 2019;111(2):219–226. doi:10.1016/j.fertnstert.2018.10.036

20. Rodríguez-Varela C, Labarta E. Clinical application of antioxidants to improve human oocyte mitochondrial function: a review. *Antioxidants*. 2020;9(12):1197. doi:10.3390/antiox9121197

21. El-Naby AAH, Ibrahim S, Hozyen HF, Sosa ASA, Mahmoud KGM, Farghali AA. Impact of nano-selenium on nuclear maturation and genes expression profile of Buffalo oocytes matured in vitro. *Mol Biol Rep*. 2020;47(11):8593–8603. doi:10.1007/s11033-020-05902-9

22. Remião MH, Lucas CG, Domingues WB, et al. Melatonin delivery by nanocapsules during in vitro bovine oocyte maturation decreased the reactive oxygen species of oocytes and embryos. *Reprod Toxicol*. 2016;63:70–81. doi:10.1016/j.reprotox.2016.05.016

23. Lin YH, Zhuang SX, Wang YL, et al. The effects of graphene quantum dots on the maturation of mouse oocytes and development of offspring. *J Cell Physiol*. 2019;234(8):13820–13831. doi:10.1002/jcp.28062

24. Abdelnour SA, Alagawany M, Hashem NM, et al. Nanominerals: fabrication methods, benefits and hazards, and their applications in ruminants with special reference to selenium and zinc nanoparticles. *Animals*. 2021;11(7):1916. doi:10.3390/ani11071916

25. Abdel-Halim B, Helmy N. Effect of nano-selenium and nano-zinc particles during in vitro maturation on the developmental competence of bovine oocytes. *Anim Prod Sci*. 2017;58. doi:10.1071/AN17057

26. Chen H, Liu C, Jiang H, et al. Regulatory role of miRNA-375 in expression of BMP15/GDF9 receptors and its effect on proliferation and apoptosis of bovine cumulus cells. *Cell Physiol Biochem*. 2017;41(2):439–450. doi:10.1159/000456597

27. Zhang M, Lu Y, Chen Y, Zhang Y, Xiong B. Insufficiency of melatonin in follicular fluid is a reversible cause for advanced maternal age-related aneuploidy in oocytes. *Redox Biol*. 2020;28:101327. doi:10.1016/j.redox.2019.101327

28. Jafarpour F, Hosseini SM, Ostadhosseini S, Abbasi H, Dalman A, Nasr-Esfahani MH. Comparative dynamics of 5-methylcytosine reprogramming and TET family expression during preimplantation mammalian development in mouse and sheep. *Theriogenology*. 2017;89:86–96. doi:10.1016/j.theriogenology.2016.10.010

29. Li B, Dewey CN. RSEM: accurate transcript quantification from RNA-Seq data with or without a reference genome. *BMC Bioinform*. 2011;12:323. doi:10.1186/1471-2105-12-323

30. Ashburner M, Ball CA, Blake JA, et al. Gene ontology: tool for the unification of biology. The Gene Ontology Consortium. *Nat Genet*. 2000;25 (1):25–29. doi:10.1038/75556

31. Kanehisa M, Goto S. KEGG: Kyoto encyclopedia of genes and genomes. *Nucleic Acids Res*. 2000;28(1):27–30. doi:10.1093/nar/28.1.27

32. Liu G, Pan B, Li S, et al. Effect of bioactive peptide on ram semen cryopreservation. *Cryobiology*. 2020;97:153–158. doi:10.1016/j.cryobiol.2020.08.007

33. Babayev E, Seli E. Oocyte mitochondrial function and reproduction. *Curr Opin Obstet Gynecol*. 2015;27(3):175–181. doi:10.1097/gco.0000000000000164

34. Zhang G, Nitteranon V, Guo S, et al. Organoselenium compounds modulate extracellular redox by induction of extracellular cysteine and cell surface thioredoxin reductase. *Chem Res Toxicol*. 2013;26(3):456–464. doi:10.1021/tx300515j

35. Lai H, Nie T, Zhang Y, et al. Selenium deficiency-induced damage and altered expression of mitochondrial biogenesis markers in the kidneys of mice. *Biol Trace Elem Res*. 2021;199(1):185–196. doi:10.1007/s12011-020-02112-z

36. Bomer N, Grote Beverborg N, Hoes MF, et al. Selenium and outcome in heart failure. *Eur J Heart Fail*. 2020;22(8):1415–1423. doi:10.1002/ejhf.1644

37. Zheng Y, Zhang B, Guan H, et al. Selenium deficiency causes apoptosis through endoplasmic reticulum stress in swine small intestine. *Biofactors*. 2021;47(5):788–800. doi:10.1002/biof.1762

38. Gheorghiu ML, Badiu C. Selenium involvement in mitochondrial function in thyroid disorders. *Hormones*. 2020;19(1):25–30. doi:10.1007/s42000-020-00173-2

39. Neal ES, Hofstee P, Askew MR, et al. Maternal selenium deficiency in mice promotes sex-specific changes to urine flow and renal expression of mitochondrial proteins in adult offspring. *Physiol Rep*. 2021;9(6):e14785. doi:10.14814/phy2.14785

40. Kaur S, Saluja M, Aniqa A, Sadwal S. Selenium attenuates bisphenol A incurred damage and apoptosis in mice testes by regulating mitogen-activated protein kinase signalling. *Andrologia*. 2021;53(3):e13975. doi:10.1111/and.13975

41. Kaur S, Maan KS, Sadwal S, Aniqa A. Studies on the ameliorative potential of dietary supplemented selenium on doxorubicin-induced testicular damage in mice. *Andrologia*. 2020;52(11):e13855. doi:10.1111/and.13855

42. Hamza RZ, Diab AEA. Testicular protective and antioxidant effects of selenium nanoparticles on Monosodium glutamate-induced testicular structure alterations in male mice. *Toxicol Rep*. 2020;7:254–260. doi:10.1016/j.toxrep.2020.01.012

43. Cao C, Zhang H, Wang K, Li X. Selenium-rich yeast mitigates aluminum-mediated testicular toxicity by blocking oxidative stress, inhibiting no production, and disturbing ionic homeostasis. *Biol Trace Elem Res*. 2020;195(1):170–177. doi:10.1007/s12011-019-01820-5

44. Baş E, Nazıroğlu M. Treatment with melatonin and selenium attenuates docetaxel-induced apoptosis and oxidative injury in kidney and testes of mice. *Andrologia*. 2019;51(8):e13320. doi:10.1111/and.13320

45. Hamza RZ, Al-Harbi MS, El-Shenawy NS. Ameliorative effect of vitamin E and selenium against oxidative stress induced by sodium azide in liver, kidney, testis and heart of male mice. *Biomed Pharmacother*. 2017;91:602–610. doi:10.1016/j.biopha.2017.04.122

46. Cao Z, Shao B, Xu F, Liu Y, Li Y, Zhu Y. Protective effect of selenium on aflatoxin b1-induced testicular toxicity in mice. *Biol Trace Elem Res*. 2017;180(2):233–238. doi:10.1007/s12011-017-0997-z

47. Bi D, Li X, Li T, et al. Characterization and neuroprotection potential of seleno-polymannuronate. *Front Pharmacol*. 2020;11:21. doi:10.3389/fphar.2020.00021

48. Wei D, Chen T, Yan M, et al. Synthesis, characterization, antioxidant activity and neuroprotective effects of selenium polysaccharide from Radix hedysari. *Carbohydr Polym*. 2015;125:161–168. doi:10.1016/j.carbpol.2015.02.029

49. Bo R, Ji X, Yang H, Liu M, Li J. The characterization of optimal selenized garlic polysaccharides and its immune and antioxidant activity in chickens. *Int J Biol Macromol*. 2021;182:136–143. doi:10.1016/j.ijbiomac.2021.03.197

50. Wang L, Li L, Gao J, et al. Characterization, antioxidant and immunomodulatory effects of selenized polysaccharides from dandelion roots. *Carbohydr Polym*. 2021;260:117796. doi:10.1016/j.carbpol.2021.117796

51. Chen W, Cheng H, Jiang Q, Xia W. The characterization and biological activities of synthetic N, O-selenized chitosan derivatives. *Int J Biol Macromol*. 2021;173:504–512. doi:10.1016/j.ijbiomac.2021.01.084

52. Zhu S, Hu J, Liu S, et al. Synthesis of Se-polysaccharide mediated by selenium oxychloride: structure features and antiproliferative activity. *Carbohydr Polym*. 2020;246:116545. doi:10.1016/j.carbpol.2020.116545

53. Gao Z, Zhang C, Tian W, et al. The antioxidative and hepatoprotective effects comparison of Chinese angelica polysaccharide (CAP) and selenizing CAP (sCAP) in CCl (4) induced hepatic injury mice. *Int J Biol Macromol*. 2017;97:46–54. doi:10.1016/j.ijbiomac.2017.01.013

54. Yue C, Chen J, Hou R, et al. The antioxidant action and mechanism of selenizing Schisandra chinensis polysaccharide in chicken embryo hepatocyte. *Int J Biol Macromol*. 2017;98:506–514. doi:10.1016/j.ijbiomac.2017.02.015

55. Yue C, Chen J, Hou R, et al. Effects of selenylation modification on antioxidative activities of schisandra chinensis polysaccharide. *PLoS One*. 2015;10(7):e0134363. doi:10.1371/journal.pone.0134363

56. Li F, Li T, Sun C, Xia J, Jiao Y, Xu H. Selenium-doped carbon quantum dots for free-radical scavenging. *Angew Chem Int Ed Engl*. 2017;56 (33):9910–9914. doi:10.1002/anie.201705989

57. Huang H, Shen Z, Chen B, et al. Selenium-doped two-photon fluorescent carbon nanodots for in-situ free radical scavenging in mitochondria. *J Colloid Interface Sci*. 2020;567:402–409. doi:10.1016/j.jcis.2020.02.011

58. Walekar LS, Zheng M, Zheng L, Long M. Selenium and nitrogen co-doped carbon quantum dots as a fluorescent probe for perfluorooctanoic acid. *Mikrochim Acta*. 2019;186(5):278. doi:10.1007/s00604-019-3400-2

59. Bueno D, Meinerz D, Waczuk E, de Souza D, Batista Rocha J. Toxicity of organochalcogens in human leukocytes is associated, but not directly related with reactive species production, apoptosis and changes in antioxidant gene expression. *Free Radic Res*. 2018;52(10):1158–1169. doi:10.1080/10715762.2018.1536824

60. Roseni Mundstock Dias G, Medeiros GR, de Lima Portella R, et al. Diphenyl diselenide modulates gene expression of antioxidant enzymes in the cerebral cortex, hippocampus and striatum of female hypothyroid rats. *Neuroendocrinology*. 2014;100(1):45–59. doi:10.1159/000365515

61. Hsieh MS, Shiao NH, Chan WH. Cytotoxic effects of CdSe quantum dots on maturation of mouse oocytes, fertilization, and fetal development. *Int J Mol Sci*. 2009;10(5):2122–2135. doi:10.3390/ijms10052122

62. Xu G, Lin G, Lin S, et al. The reproductive toxicity of CdSe/ZnS quantum dots on the in vivo ovarian function and in vitro fertilization. *Sci Rep*. 2016;6:37677. doi:10.1038/srep37677

63. Liu N, Tang M. Toxicity of different types of quantum dots to mammalian cells in vitro: an update review. *J Hazard Mater*. 2020;399:122606. doi:10.1016/j.jhazmat.2020.122606

64. Amani Abkenari S, Safdarian L, Amidi F, et al. Metformin improves epigenetic modification involved in oocyte growth and embryo development in polycystic ovary syndrome mice model. *Mol Reprod Dev*. 2021;88(12):817–829. doi:10.1002/mrd.23537

65. Yan K, Cui K, Nie J, et al. Mogroside V protects porcine oocytes from lipopolysaccharide-induced meiotic defects. *Front Cell Dev Biol*. 2021;9:639691. doi:10.3389/fcell.2021.639691

66. Jia L, Zeng Y, Hu Y, et al. Homocysteine impairs porcine oocyte quality via deregulation of one-carbon metabolism and hypermethylation of mitochondrial DNA†. *Biol Reprod*. 2019;100(4):907–916. doi:10.1093/biolre/ioy238